Activation of Cholera Toxin Production by Anaerobic Respiration of Trimethylamine N-oxide in *Vibrio cholerae*[*]

Kang-Mu Lee[‡1], **Yongjin Park**[‡1], **Wasimul Bari**[‡], **Mi Young Yoon**[‡], **Junhyeok Go**[‡], **Sang Cheol Kim**[§], **Hyung-il Lee**[¶], **and Sang Sun Yoon**[‡||**2]

*From the ‡Department of Microbiology and Immunology, Brain Korea 21 Project for Medical Sciences, ||Institute for Immunology and Immunological Diseases, and **Research Institute of Bacterial Resistance, §Department of Otorhinolaryngology, Yonsei University College of Medicine, Seoul, 120-752 Korea and the ¶Department of Chemistry, University of Ulsan, Ulsan 680-749, Korea*

Background: The human intestine, in which *Vibrio cholerae* exerts its virulence, is an anaerobic environment.
Results: When grown anaerobically with trimethylamine N-oxide (TMAO), *V. cholerae* exhibited enhanced growth and cholera toxin (CT) production was remarkably induced.
Conclusion: Anaerobic TMAO respiration may serve as a signal to increase *V. cholerae* virulence.
Significance: A novel growth condition that induces CT production is uncovered.

Vibrio cholerae is a Gram-negative bacterium that causes cholera. Although the pathogenesis caused by this deadly pathogen takes place in the intestine, commonly thought to be anaerobic, anaerobiosis-induced virulence regulations are not fully elucidated. Anerobic growth of the *V. cholerae* strain, N16961, was promoted when trimethylamine N-oxide (TMAO) was used as an alternative electron acceptor. Strikingly, cholera toxin (CT) production was markedly induced during anaerobic TMAO respiration. N16961 mutants unable to metabolize TMAO were incapable of producing CT, suggesting a mechanistic link between anaerobic TMAO respiration and CT production. TMAO reductase is transported to the periplasm via the twin arginine transport (TAT) system. A similar defect in both anaerobic TMAO respiration and CT production was also observed in a N16961 TAT mutant. In contrast, the abilities to grow on TMAO and to produce CT were not affected in a mutant of the general secretion pathway. This suggests that *V. cholerae* may utilize the TAT system to secrete CT during TMAO respiration. During anaerobic growth with TMAO, N16961 cells exhibit green fluorescence when stained with 2′,7′-dichlorofluorescein diacetate, a specific dye for reactive oxygen species (ROS). Furthermore, CT production was decreased in the presence of an ROS scavenger suggesting a positive role of ROS in regulating CT production. When TMAO was co-administered to infant mice infected with N16961, the mice exhibited more severe pathogenic symptoms. Together, our results reveal a novel anaerobic growth condition that stimulates *V. cholerae* to produce its major virulence factor.

Cholera is an acute noninflammatory diarrheal disease that affects humans infected with the causative pathogen *Vibrio cholerae* (1). Cholera has been involved in seven historic pandemics and has posed a huge threat to human health in regional epidemics until very recently (2). Among more than 200 *O*-antigen serotypes, O1 and O139 serotypes are toxigenic and can cause cholera. O1 serotype strains are further classified into two biotypes, El Tor and Classical, the latter of which is presumed extinct (3). Invading *V. cholerae* cells that survive the acidic gastric environment enter the intestine, where they produce an array of virulence factors, including cholera toxin (CT)[3] and toxin co-regulated pilus (TCP) (4). CT is an ADP ribosylating toxin that creates imbalanced ion transport across the intestinal epithelia leading to loss of electrolytes and water from the epithelial cells (5). TCP is known to play an essential role in the bacterial colonization to the intestinal surface (6). Human intestine is occupied with commensal bacteria, most of which are strict anaerobes (7). This suggests that (i) the microenvironment in the human intestine is anaerobic and (ii) anaerobiosis may serve as a host factor that modulates *V. cholerae* virulence (8). Consistent with this notion, recent reports showed that under anaerobic conditions, expression of *tcpP*, a regulator of virulence gene expression (9) was elevated and this increase was mediated by a novel oxygen sensing mechanism of AphB, a LysR-type transcriptional activator (10, 11). These findings were achieved from *V. cholerae* cells grown anaerobically in AKI media.

As a facultative anaerobe, *V. cholerae* can support its growth by fermentation of diverse carbohydrates including glucose, sucrose, maltose, mannitol, lactose, dextrin, and starch (12, 13). Sucrose fermentation has been used as a basis for the identification of *V. cholerae* species among fecal isolates (14). However, whether *V. cholerae* can also support anaerobic growth by respiration of alternative electron acceptors (AEAs) has not been

[1] Both authors contributed equally to this work.
[2] To whom correspondence should be addressed: Dept. of Microbiology and Immunology, Yonsei University College of Medicine, 250 Seongsanno, Seodaemun-gu Seoul 120-752, Korea, Tel.: 82-2-2228-1824; Fax: 82-2-392-7088; E-mail: sangsun_yoon@yuhs.ac.

[3] The abbreviations used are: CT, cholera toxin; TMAO, trimethylamine N-oxide; TMA, trimethylamine; DCF-DA, 2′,7′-dichlorofluorescein diacetate; AEA, alternative electron acceptors; DMSO, dimethyl sulfoxide; DIC, differential interference contrast; Tn, transposon; TAT, twin arginine transport; NAC, N-acetylcysteine; TCP, toxin co-regulated pilus.

TABLE 1
Bacterial strains and plasmid used in this study

Strains or plasmids	Relevant characteristics	Ref. or source
V. cholerae strains		
N16961	O1, El Tor	Lab collection
N16961 P_{ctxAB}::lacZ fusion	*ctxAB* promoter lacZ fusion construct	This study
$\Delta VC1720$	N16961, *VC1720*::TnKGL3	This study
$\Delta VC0116$	N16961, *VC0116*::TnKGL3	This study
$\Delta VC2053$	N16961, *VC2053*::TnKGL3	This study
$\Delta VC1024$	N16961, *VC1024*::TnKGL3	This study
N16961 Δ*tat* mutant	N16961, *VC0086-VC0088* deleted	This study
N16961 Δ*sec* mutant	N16961, *VC0742-VC0744* deleted	This study
N16961 Δ*type II* mutant	N16961, *VC2723-VC2734* deleted	This study
O395	O1, Classical	Lab collection
C6706	O1. El Tor	Lab collection
569B	O1, Classical	Lab collection
MO10	O139	Lab collection
AM19226	Non-O1, non-O139	Lab collection
CVD115	*hap, rtxA* double mutant of CVD110	(24)
E. coli strain		
SM10/λ*pir*	Km^r *thi-1 thr leu tonA lacY supE recA*::RP4–2-Tc::Mu *pir$^+$*, for conjugal transfer	Lab collection
Plasmids		
pCVD442	*sacB* suicide vector from plasmid pUM24	Lab collection
pVIK112	Suicide vector for *lacZ* reporter fusion, Km^r	Lab collection
pTnKGL3	Suicide vector bearing TnKGL3, Cm^r Km^r	Lab collection

extensively studied. In addition, studies have not been conducted on (i) which AEA can most efficiently stimulate anaerobic growth of *V. cholerae*, (ii) how anaerobic respiration contributes to bacterial proliferation in the human intestine, and (iii) how *V. cholerae* virulence is regulated under such anaerobic respiratory growth.

The genome of the 7th pandemic strain N16961 contains several genes that are likely involved in anaerobic respiration. It appears that N16961 is capable of utilizing fumarate, nitrate, trimethylamine N-oxide (TMAO), or dimethyl sulfoxide (DMSO) as AEAs (15). In this study, we investigated the anaerobic growth and virulence regulation of N16961 under diverse anaerobic respiration conditions. N16961 grew better and secreted remarkably high amounts of CT while growing anaerobically with TMAO. We also uncovered the possible mechanisms for enhanced CT production and explored the potential *in vivo* relevance of anaerobic TMAO respiration. This report reveals novel features associated with *V. cholerae* virulence during a growth mode that may occur inside the human intestine.

EXPERIMENTAL PROCEDURES

Ethics Statement—All animal experiments were conducted following the national guidelines provided by the Korean government (Ministry for Food, Agriculture, Forestry and Fisheries) and in strict accordance with the institutional guidelines for animal care and use of laboratory animals. The methods for animal experimentations using infant mice were approved by the Committee on the Ethics of Animal Experiments of the Yonsei University College of Medicine (permit number 2011-0166).

Bacterial Strains and Growth—Bacterial strains and plasmids used in this study are listed in Table 1. Bacterial cultures were grown at 37 °C in Luria-Bertani media (LB, 10 g of tryptone, 5 g of yeast extract, and 10 g of NaCl/liter). The anaerobic growth of *V. cholerae* strains was performed as described elsewhere (16). To support anaerobic growth, trimethylamine N-oxide, dimethyl sulfoxide, or fumarate (Sigma) was added to the medium and termed LBT, LBD, or LBF, respectively.

CT ELISA and Western Blot Analysis—CT ELISA was performed as previously described (17). Purified CT (List Biological Laboratories, Inc., Campbell, CA) was used to provide a standard curve. For Western blot analysis, culture supernatants were first concentrated via TCA (trichloroacetic acid, Sigma) precipitation (18). Western blot analysis was carried out as previously described (19). Rabbit polyclonal antibody raised against CT subunit B (Abcam Inc., Cambridge, UK) was used for both assays.

Transposon (Tn) Mutant Screening—A library of Tn-insertion mutants was constructed by the conjugal transfer of TnKGL3, a mariner-based Tn (3). Km^r mutants (>20,000) were screened for their capability to grow anaerobically on LB agar plates containing 50 mM TMAO. N16961 mutants found to form smaller-sized colonies after 2 days of anaerobic growth were selected and individually tested in broth cultures. Arbitrary PCR was performed to determine the location of the Tn insertion site. Information regarding primer sequences and PCR protocol are described elsewhere (3).

Construction of Mutants and ctxAB Promoter-lacZ Fusion Strain—*V. cholerae* mutants were created by allele replacement as previously described (20). The 500-base pair flanking sequences located at both ends to introduce mutation were amplified by PCR with the primers listed in Table 2. Construction of a single-copy P_{ctxAB}::*lacZ* transcriptional fusion and β-galactosidase activity assay were performed as described previously (3).

Confocal Microscope—Differential interference contrast (DIC) and green fluorescent images were acquired using a confocal laser scanning microscope (FV-1000; Olympus Optical Co. Ltd., Japan) and its operating software, FV10-ASW (version 02.01). Detailed procedures are described elsewhere (16, 21). For ROS detection, N16961 was grown anaerobically for 8 h with 50 mM TMAO, DMSO, or fumarate. Aliquots of each culture were removed and stained with 10 μM DCF-DA (2′,7′-dichlorofluorescein diacetate, Sigma) for 30 min. To capture the green fluorescence, samples were scanned at 488 nm and

TABLE 2
Primers used in this study

Gene name	Direction[a]	Primer sequence (5'-3')[b]
Cloning		
ctxA-promoter fusion	F	CACAT<u>GAATT</u>CACTATCGAGTCAGAGCAATCCG
ctxA-promoter fusion	R	ATTGG<u>TCTAGA</u>TTGTTTAACAGAAAAATAATTGATCAAAAC
tatABC Left	F	CTCTA<u>GTCGAC</u>ACTGCTGTATGTCGAAGGCTTGG
tatABC Left	R	GAATT<u>GAGCTC</u>GATAAGAAGTTGCCAAATACTGATACCACC
tatABC Right	F	CACTA<u>GAGCTC</u>CAAGCGTCCATACATTATCGTTGGTG
tatABC Right	R	GAATT<u>CCCGGG</u>TCAGCGAGGTAAGAACGACTTTCATAA
yajC-secD-secF Left	F	AACCT<u>GTCGAC</u>GGTGTGCGTCGTGGTATCGACA
yajC-secD-secF Left	R	GATAT<u>GAGCTC</u>CGCCTGCGGCATGTGCTACAGAA
yajC-secD-secF Right	F	AACCT<u>GAGCTC</u>AATGATCCACGGTTTTGCGCTG
yajC-secD-secF Right	R	GATAT<u>CCCGGG</u>CCTTGGGATATGGCTGCAGGTG
VC2734-VC2723[c] Left	F	AACCT<u>GTCGAC</u>AACGTTTGAGACACTTCGCTCCACT
VC2734-VC2723 Left	R	GATAT<u>GAGCTC</u>TTTGCGCATCATTACTCGCCAC
VC2734-VC2723 Right	F	AACCT<u>GAGCTC</u>TGCCAAGAGAGCGTTGTGACCC
VC2734-VC2723 Right	R	GATAT<u>CCCGGG</u>TGGGCTCTGCAGCACTGAAAGC
qRT-PCR		
rpoD	F	AGGCAGTGGCTCACGACCCAT
rpoD	R	ATGCGACTTGGTGGATCCGTCA
ctxB	F	CCTCAGGGTATCCTTCATCCT
ctxB	R	GTGCAGAATACCACAACACAC
ctxA	F	ACGGCTCTTCCCTCCAAGCTCT
ctxA	R	GGTATCGAGTTCATTTTGGGGTGC
toxT	F	GCTGTCCTTTCTGAAGTGGTAA
toxT	R	CTGCCCAACGCCAATTACGCCGT
toxR	F	ATTGGCTGGCTGCGGTGTGTTC
toxR	R	TTGATCGCCCGAGTGGAAACG
tcpP	F	GAGCGGATAAAAATTGAGTGGGGGA
tcpP	R	CCCCGGTAACCTTGCTAAATCTCGT

[a] F, forward; R, reverse.
[b] Restriction enzyme recognition sequences are underlined.
[c] *VC2734-VC2723* are genes encoding components of Type II secretion system.

emission was detected through a 520-nm band filter. The DIC and green fluorescence images were collected simultaneously.

Two-dimensional Gel Electrophoresis and Protein Identification—N16961 cells grown anaerobically for 16 h in LB, LBT, LBD, or LBF were harvested by centrifugation at 14,000 × *g* for 5 min. The cell pellet was washed three times with ice-cold PBS and submitted to Genomine Inc. (Pohang, Korea), where the entire proteomic analysis was performed.

Infant Mouse Infection—Infant mice (~5 to 6 days old, Central Lab Animal Inc., Seoul) were orogastrically infected with *V. cholerae* strains following procedures previously described (3). After 24 h infection, intestinal homogenates were prepared and the number of viable cells was determined by spreading serial diluents on LB agar containing Sm (for total bacterial cell count) or LB agar containing both Sm and Km (for Δ*torD* mutant).

qRT-PCR—Transcript levels of virulence-associated genes (*ctxA*, *ctxB*, *toxT*, *toxR*, and *tcpP*) were measured by qRT-PCR. The detailed analysis procedure has been described previously (21). Transcript levels of the *rpoD* gene were used to normalize the transcript levels of the tested genes. The primers used for qRT-PCR are listed in Table 2.

TMAO Reductase Activity Assay—*V. cholerae* strains, N16961, and four Tn-insertion mutants, were grown anaerobically in LB or LBT for 16 h. To analyze the TMAO reductase activity in different cellular fractions, the periplasmic and cytoplasmic fractions were separated by polymyxin B treatment. Cell pellets were resuspended with PBS containing 2,000 units of polymyxin B and incubated for 15 min at 4 °C. After incubation, reaction mixtures were centrifuged at 12,000 rpm for 10 min and the supernatants were saved for periplasmic fractions. Cell pellets were then resuspended in PBS and sonicated to

produce cytoplasmic fractions. Equal amounts of proteins present in each fraction were resolved by a 9% nondenaturing polyacrylamide gel, and a native gel-based enzyme assay was performed as previously described (22).

Statistical Analysis—Data are expressed as mean ± S.D. An unpaired Student's *t* test was used to analyze the data. A *p* value of <0.05 was considered statistically significant. All experiments were repeated for reproducibility.

RESULTS

Anaerobic Growth of the V. cholerae Strain N16961 Was Enhanced by TMAO Respiration and CT Production Was Remarkably Induced under Such Conditions—*V. cholerae* was reported to support anaerobic growth by using diverse AEAs, such as TMAO, fumarate, and DMSO (15). To examine the relative anaerobic growth achieved using each AEA, N16961 was grown in LB supplemented with TMAO, fumarate, or DMSO at three different concentrations. As shown in Fig. 1*A*, bacterial growth was enhanced when grown with TMAO or fumarate. When TMAO was added at 50 mM concentration, the final A_{600} values were ~2-fold higher than that of control growth in plain LB media (*black bar to the left*). N16961 also exhibited better anaerobic growth using fumarate with the growth enhancement being as robust as what was observed in TMAO-amended LB broth. Additional increases in the final A_{600} values were not observed when DMSO was used.

The level of CT secreted to culture supernatants during each anaerobic culture was then measured. Surprisingly, CT production was strikingly induced during TMAO-stimulated anaerobic respiratory growth (Fig. 1*B*). Such a dramatic induction was not detected in other types of anaerobic growth. Notably, CT was not produced when N16961 was grown aerobically with

equal amounts of TMAO (Fig. 1*B*), demonstrating that TMAO-induced CT production occurred only under anaerobic growth conditions. To confirm the CT ELISA results, Western blot analysis was also performed using an antibody against CT subunit B. As shown in Fig. 1*C*, the band specific to CT subunit B was only detected in the cell-free culture supernatant of N16961 grown by anaerobic TMAO respiration. These results suggest that among various AEAs, TMAO can most efficiently stimulate anaerobic growth of the *V. cholerae* strain N16961. In addition, CT production is specifically and substantially induced during TMAO respiration.

The study also investigated whether TMAO-stimulated CT production was reflected in the transcriptional activation of CT-coding genes. To address this, the promoter activity of *ctxAB* genes was monitored by constructing a chromosomal *lacZ* reporter fusion to this promoter. Consistent with the CT ELISA results, a significant level of β-galactosidase activity was detected only in N16961 grown anaerobically in LB containing 50 mM TMAO (Fig. 1*D*). The mRNA expression levels of other virulence-associated genes were then measured by qRT-PCR analysis. Transcript levels of five selected genes, *ctxA*, *ctxB*, *toxT*, *toxR*, and *tcpP*, invariably increased in N16961 grown in LBT compared with LB (Fig. 1*E*). Expression of *ctxA* and *tcpP* was up-regulated to the highest level at greater than ~50-fold, whereas the mRNA levels of *ctxB*, *toxT*, and *toxR* increased ~13-, ~17-, and ~12-fold, respectively (Fig. 1*E*).

The 7th pandemic *V. cholerae* strain N16961 is classified as O1 serogroup and El Tor biotype (23). We therefore asked whether the mechanism of TMAO-stimulated CT production is conserved among other types of *V. cholerae* strains. Two different Classical biotype strains (O395 and 569B) and another O1 El Tor biotype strain (C6706) produced comparable CT levels under the same anaerobic growth conditions (Fig. 1*F*). Interestingly, both the O139 serogroup strain MO10 and the non-O1/non-O139 strain AM19226 failed to produce CT. As expected, CT was not produced in the CVD115 strain derived from CVD110 that has deletions in CT-coding genes (24) or in the N16961 strain grown in plain LB (leftmost lane). Although only a limited number of *V. cholerae* strains were tested, these results may suggest that the mechanism for producing CT during TMAO respiration is conserved in *V. cholerae* O1 serogroup strains.

CT Production Was Not Observed in N16961 Tn Insertion Mutants with Defects in Their Ability to Respire TMAO—To examine whether a mechanistic link exists between enhanced anaerobic growth by TMAO respiration and CT production, an N16961 Tn random insertion mutant library was constructed and screened for mutants that failed to form colonies with a larger size in LB-agar plates supplemented with 50 mM TMAO. In four mutants that were recovered, it was clearly shown that the presence of TMAO did not increase their anaerobic growth (Fig. 2*A*). In all of these mutants, the final A_{600} values after 16 h of anaerobic culture in LBT were similar to those obtained from LB growth. Arbitrary PCR amplification followed by DNA sequencing analysis demonstrated that Tn was inserted in the protein coding regions of *VC1720*, *VC0116*, *VC2053*, or *VC1024*, respectively (Fig. 2*B*). *VC1720*, termed *torD*, encodes a chaperone protein for TorA (VC1692), a major subunit of the
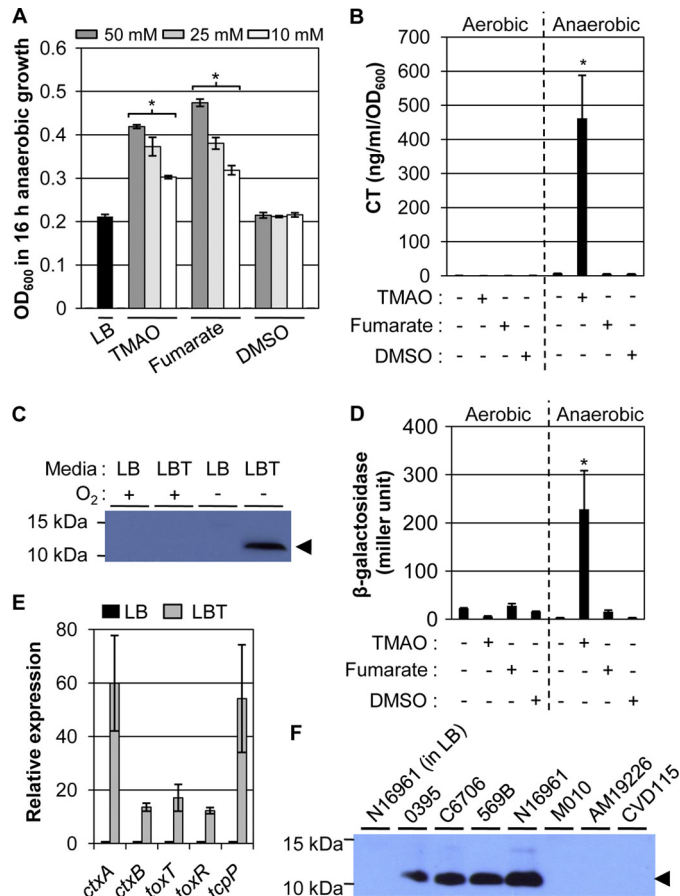

FIGURE 1. **CT production is specifically induced during anaerobic growth by TMAO respiration in N16961.** *A,* anaerobic growth of N16961 in the presence of AEAs. Bacterial cells precultured aerobically in LB were inoculated to LB media or to LB containing TMAO, fumarate, or DMSO and grown statically inside the anaerobic chamber for 16 h. To examine dose dependence, three different concentrations (50, 25, and 10 mM) of TMAO, fumarate, and DMSO were used. Three independent experiments were performed and values of mean ± S.D. are displayed in each *bar.* *, $p < 0.01$ *versus* A_{600} values of N16961 after anaerobic growth in plain LB. *B,* the effect of anaerobiosis and the presence of AEAs on CT production. N16961 was aerobically or anaerobically grown in LB with each AEA (50 mM) for 16 h. The CT level was determined by ELISA. *, $p < 0.001$ *versus* CT levels from other cultures. *C,* Western blot analysis of culture supernatants harvested from aerobic or anaerobic growth of N16961 in LB or LBT (LB + 50 mM TMAO). Prior to loading onto SDS-PAGE gel, each culture supernatant was concentrated by TCA precipitation. The protein band that corresponds to the CT subunit B was shown with an *arrowhead.* *D,* promoter activity of *ctxAB* genes in N16961 grown under the indicated culture conditions. An N16961 reporter strain harboring single-copy P$_{ctxAB}$::*lacZ* fusion was assayed in triplicate for β-galactosidase activity. Values of mean ± S.D. are presented. *, $p < 0.001$ *versus* β-galactosidase activity measured from other cultures. *E,* qRT-PCR analysis of *V. cholerae* virulence-associated genes. qRT-PCR was conducted on cDNA synthesized from 2 μg of total RNA extracted from N16961 grown anaerobically either in LB (*black bars*) or in LBT (*gray bars*). Bacterial cells were harvested after 8 h of growth and subjected to RNA isolation. Transcript levels of the tested genes indicated at the *bottom* were normalized with those of the *rpoD* gene transcript. Three independent experiments were performed and values of mean ± S.D. are displayed in each *bar.* The primers used for qRT-PCR are listed in Table 2. *, $p < 0.05$ *versus* transcript levels in N16961 grown in LB. *F,* Western blot analysis of CT subunit B in a variety of *V. cholerae* strains. Bacterial strains were grown anaerobically in LBT (except for the first lane; N16961 grown in LB) for 16 h and culture supernatants, concentrated via TCA precipitation, were loaded onto SDS-PAGE for Western blot analysis. Information on bacterial strains was provided in Table 1. The protein band that corresponds to the CT subunit B was shown with an *arrowhead.*

TMAO reductase complex (25). VC0116 (HemN) is an oxygen-independent coproporphyrinogen III oxidase involved in heme biosynthesis (26, 27). *VC2053* encodes a heme chaperone for
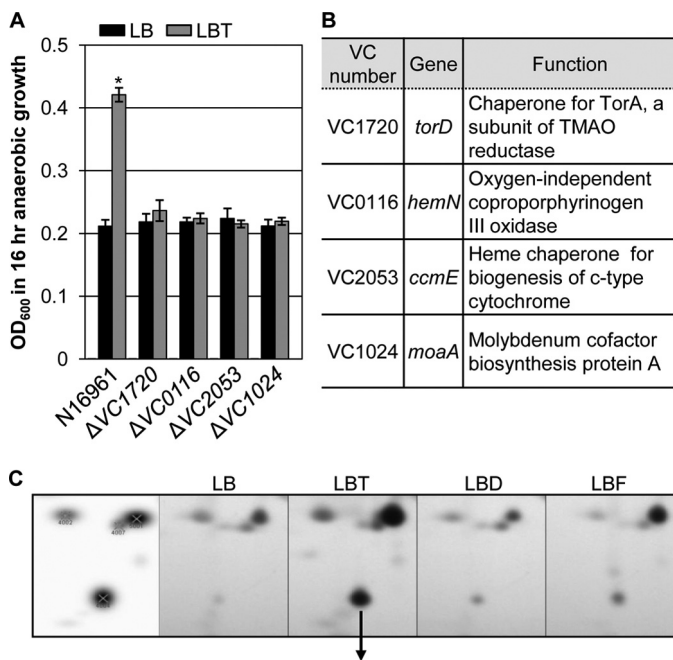
FIGURE 2. **Identification of N16961 mutants defective in anaerobic growth by TMAO respiration.** *A,* anaerobic growth of wild type N16961 and four different mutants recovered from screening Tn mutant library. Strains were grown anaerobically in LB (*black bars*) or LBT (*gray bars*) for 16 h, and values of A_{600} (mean ± S.D., $n = 3$) are displayed. *, $p < 0.001$ *versus* A_{600} values of other cultures. *B,* information of genes disrupted in each mutant and function of the proteins encoded from each gene. *C,* up-regulated synthesis of VC1025 protein in N16961 grown in LBT. Bacterial proteins were extracted from N16961 grown anaerobically in LB, LBT, LBD (LB + 50 mM DMSO), or LBF (LB + 50 mM fumarate) and were separated in two-dimensional gels. The same area of each gel containing a spot for VC1025 was compared. The VC1025 protein was identified by Q-TOF. The *leftmost image* represents protein spots detected by gel image analysis.

FIGURE 3. **TMAO reductase activity detected in the recovered mutants and their capabilities to produce CT.** *A,* strains indicated at the *bottom* were grown anaerobically in LB or in LBT for 16 h. Proteins present in cytoplasmic (*C*) and periplasmic (*P*) fractions were separated by native gel and stained for TMAO reductase activity. One μg of protein was subjected to native gel electrophoresis and activity staining in each lane. The activity staining was performed as described under "Experimental Procedures." *B,* CT ELISA analysis of mutant strains. Experimental conditions were identical to those described in the legend to Fig. 1*B*. *, $p < 0.001$ *versus* CT levels from other cultures.

biosynthesis of the c-type cytochrome that is required for active TMAO reductase (15). TMAO reductase is also featured with the presence of a molybdenum cofactor (28). A mutant of *VC1024* (*moaA*) that is defective in the machinery required to synthesize the molybdenum cofactor was included among the mutants incapable of utilizing TMAO under anaerobic conditions. Consistent with this finding, the synthesis of molybdenum cofactor biosynthesis protein B produced from a gene (*VC1025*, *moaB*) clustered as an operon with *moaA* was specifically up-regulated in LBT-grown N16961 in two-dimensional gel electrophoresis analysis (Fig. 2*C*).

The TMAO reductase activity in each mutant was then measured by a native gel-based assay (22). As expected, TMAO reductase activity was robustly induced in N16961 grown anaerobically in LBT, but not in LB (Fig. 3*A*). TMAO reductase was detected in both the periplasm and cytoplasmic space in LBT-grown N16961. TMAO reductase was non-detectable in the Δ*VC1720* and Δ*VC1024* mutants, whereas its activity was significantly decreased in the Δ*VC0116* and Δ*VC2053* mutants (Fig. 3*A*). These results further confirm that the incapability of these mutants to exhibit enhanced anaerobic growth using TMAO is indeed caused by the presence of defective TMAO reductase.

We then examined whether or not these mutants have compromised capabilities to produce CT. As shown in Fig. 3*B*, the
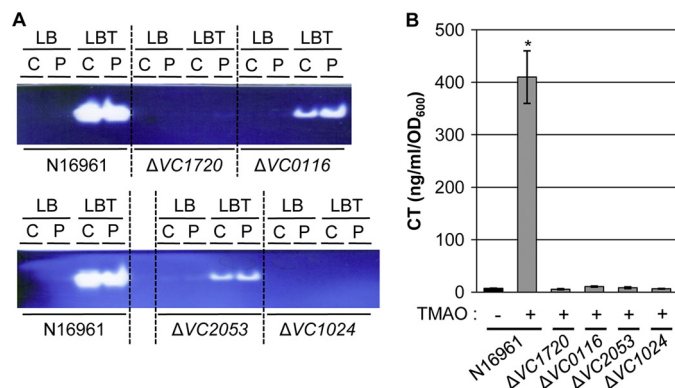
CT levels induced in all of these mutant strains were negligible during anaerobic growth with TMAO, whereas robust CT production was observed in the wild type strain N16961. Together, our results demonstrate that (i) the ability to produce heme group, cytochrome *c*, and molybdenum cofactor is necessary to produce functionally intact TMAO reductase and (ii) that CT production during anaerobiosis occurs in strict association with TMAO respiration.

The Twin Arginine Transport Pathway Was Required for Both TMAO Respiration and CT Production—TMAO reductase is active in the periplasmic space and is transported to the periplasm via the twin arginine transport (TAT) system in *Escherichia coli* (29). The bacterial TAT system is an inner membrane-associated apparatus for protein translocation that can export cytoplasmic proteins containing a consensus twin arginine recognition motif in its N terminus (30). To elucidate whether TMAO reductase of *V. cholerae* is also processed in a similar way, we first analyzed the primary sequence of TMAO reductase, the product of *torA* gene (*VC1692*). As shown in Fig. 4*A*, TMAO reductase of *V. cholerae* strain N16961 also harbors the twin arginine motif in its N-terminal region, suggesting that this enzyme is likely a substrate of the TAT system. Unlike *E. coli*, in which the *torA, torC,* and *torD* genes are clustered as an operon (31), the *torD* gene is located in a separate region of the N16961 genome (Fig. 4*A*). TorC is a cytochrome *c*-type subunit of TMAO reductase (32).

We then constructed a Δ*tat* mutant in which three genes (*tatA, tatB,* and *tatC*) of the TAT operon were deleted and tested whether such a mutant can exhibit enhanced anaerobic growth on TMAO. As shown in Fig. 4*B*, no growth enhancement was observed in the Δ*tat* mutant in response to the presence of TMAO, demonstrating that the TAT system is critically required for activation of the TMAO reductase in *V. cholerae*. Importantly, CT was not produced in the Δ*tat* mutant during anaerobic growth in LBT (Fig. 4*C*). This result further suggests that CT production is specifically induced only under conditions in which bacterial anaerobic growth is stimulated by TMAO respiration.
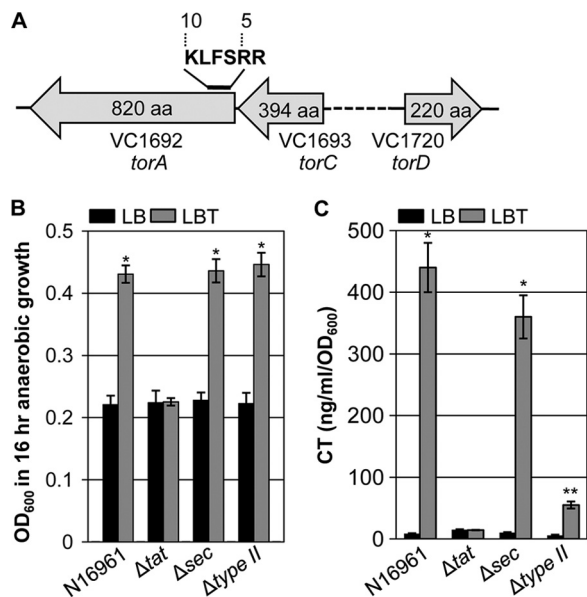
FIGURE 4. **Involvement of the TAT pathway in anaerobic TMAO respiration and CT production.** *A*, chromosomal location of *torA*, *torC,* and *torD* genes is depicted. Twin arginine recognition motif in the N-terminal region of the TorA protein is indicated. *B*, anaerobic growth of N16961, Δ*tat*, Δ*sec*, and Δ*type II* mutant strains in LB (*black bars*) or LBT (*gray bars*). Experimental conditions were identical to those described in the legend to Fig. 1*A*. Three independent experiments were performed and values of mean ± S.D. are displayed in each *bar*. *, $p < 0.01$ *versus* A_{600} values obtained from growth in plain LB. *C*, CT production of N16961, Δ*tat*, Δ*sec,* and Δ*type II* mutant strains grown in LB (*black bars*) or LBT (*gray bars*). Experimental conditions were identical to those described in the legend to Fig. 1*B*. *, $p < 0.001$; **, $p < 0.01$ *versus* CT levels detected in cell-free supernatants harvested from LB grown cells.

It is well established that CT is secreted into the environmental milieu from the periplasmic space via a type II secretion system (T2SS) in *V. cholerae* (33, 34). For facilitated transport across the inner membrane into the periplasm, CT is targeted to either the general secretion pathway (SEC) (35, 36) or the TAT system (22). For this reason, we also examined the effects of SEC or T2SS deficiency on anaerobic TMAO respiration and CT secretion. The ability to support anaerobic growth by TMAO respiration was not affected in N16961 Δ*sec* and Δ*type II* mutants, respectively (Fig. 4*B*). The extent to which anaerobic growth was increased by TMAO respiration in each of these two mutants was almost identical to that observed in N16961. The CT level detected in cell-free culture supernatants of the Δ*sec* mutant was only mildly decreased. As anticipated, CT production was substantially decreased in the Δ*type II* mutant grown anaerobically in LBT (Fig. 4*C*), further verifying that T2SS is the predominant route for CT secretion to the environment. These results also suggest that the TAT system plays a more important role than SEC in CT secretion during anaerobic growth with TMAO.

Reactive Oxygen Species (ROS) Is Produced during TMAO Respiration whereas CT Production Was Antagonized by the Presence of N-Acetylcysteine, a ROS Scavenger—During TMAO reduction to TMA, an oxygen atom is liberated from TMAO via a reaction that involves the oxidation of a molybdenum cofactor present in the TorA subunit (37–39). Hence, we hypothesized that ROS might be generated during this reaction. To address this issue, N16961 cells grown in various culture media

were stained with DCF-DA, a fluorescent dye that reacts specifically with ROS (40). Fig. 5, *A–D*, shows confocal images of N16961 grown anaerobically in LB, LBT, LBF, or LBD, respectively. The first image in each panel is a merged DIC and fluorescent image, whereas the second is a green fluorescent image. The green fluorescence signal was only faintly visible in N16961 cells grown in LB, suggesting that ROS is minimally produced during anaerobic growth in LB (Fig. 5*A*). The fluorescent signal in cells grown in LBD was comparable with that detected in LB-grown N16961 cells (Fig. 5*D*), whereas the signal was not detectable in cells grown in LBF (Fig. 5*C*). Importantly, a large population of LBT-grown cells produced fluorescent signals that were significantly more intense than those detected in other groups (Fig. 5*B*). Together, these results suggest that ROS is likely produced as a result of TMAO respiration. The results provide strong clues that this undesirable by-product may trigger a cellular mechanism that leads to CT production in N16961.

Next, we tested the effect of *N*-acetylcysteine (NAC), a ROS scavenger, on CT production and *ctxAB* promoter activity. In the presence of increasing amounts of NAC, the CT level induced during anaerobic growth by TMAO respiration was gradually decreased (Fig. 6*A*). Likewise, a clear dose-dependent decrease was also observed in the P_{ctxAB} activity (Fig. 6*B*). These results suggest that ROS availability can regulate the degree of *ctxAB* gene expression and CT production. We then investigated whether the CT production level is elevated by exogenous addition of H_2O_2. When N16961 was grown anaerobically in LB media that contained increasing concentrations of TMAO, CT production was gradually increased (Fig. 6*C*, *black bars*). The level of CT produced during TMAO respiration significantly increased in the presence of 100 μM H_2O_2 (Fig. 6*C*, *gray bars*). During anaerobic growth with 20 or 30 mM TMAO, CT production increased by ~1.8- or ~1.9-fold, respectively, with the addition of 100 μM H_2O_2. When grown with 40 or 50 mM TMAO, CT production increased ~1.5-fold in the presence of H_2O_2 compared with growth in its absence. Notably, CT production was not induced by H_2O_2 when bacterial cells were grown in plain LB (Fig. 6*C*, *leftmost set of bars*). In addition, H_2O_2–mediated stimulation of CT production was not observed when fumarate or DMSO were used to support anaerobic growth of N16961 (Fig. 6, *D* and *E*). These results suggest that H_2O_2, an exogenously added ROS, can promote CT production only when *V. cholerae* cells grow by anaerobic TMAO respiration.

When Infected with TMAO, the Cytotoxicity Exerted by V. cholerae Strains Was Elevated in Infant Mouse Intestine—Finally, we sought to examine the effect of TMAO on *in vivo* virulence using an infant mouse model of *V. cholerae* infection. We first measured the fluid accumulation induced by orogastric challenge of *V. cholerae* N16961 cells (2×10^6 cells). Higher levels of the intestinal fluid accumulation ratio were observed in mice infected with bacterial cells re-suspended in LB + 100 mM TMAO (fluid accumulation ratio > ~0.12) than in mice infected with bacterial suspensions that contain no TMAO (fluid accumulation ratio > ~0.08) (Fig. 7*A*). Importantly, mice infected with extraneously added TMAO exhibited higher susceptibility in response to intestinal infection. Although all of the
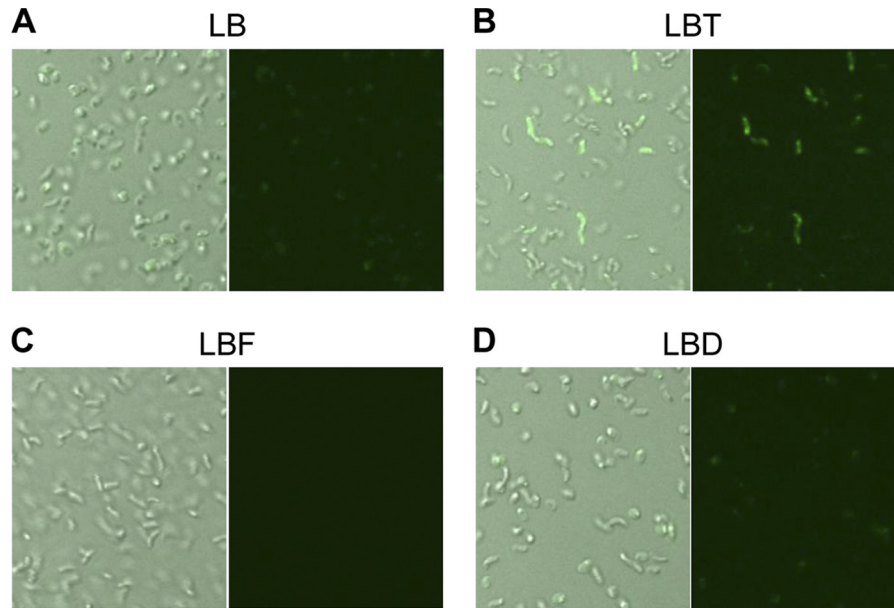
FIGURE 5. **ROS is spontaneously generated during anaerobic TMAO respiration.** Confocal microscope images of N16961 grown anaerobically in LB (*A*), LBT (*B*), LBF (*C*), and LBD (*D*). LBF and LBD indicate LB + 50 mM fumarate and LB + 50 mM DMSO, respectively. *Left images* in each panel represent merged DIC and green fluorescent images, whereas *right images* represent only green fluorescent images. Bacterial cells grown in each media for 8 h were strained with 10 μM DCF-DA for 30 min and processed for confocal microscopic analysis. Images were acquired at $\times$1,000 magnification.
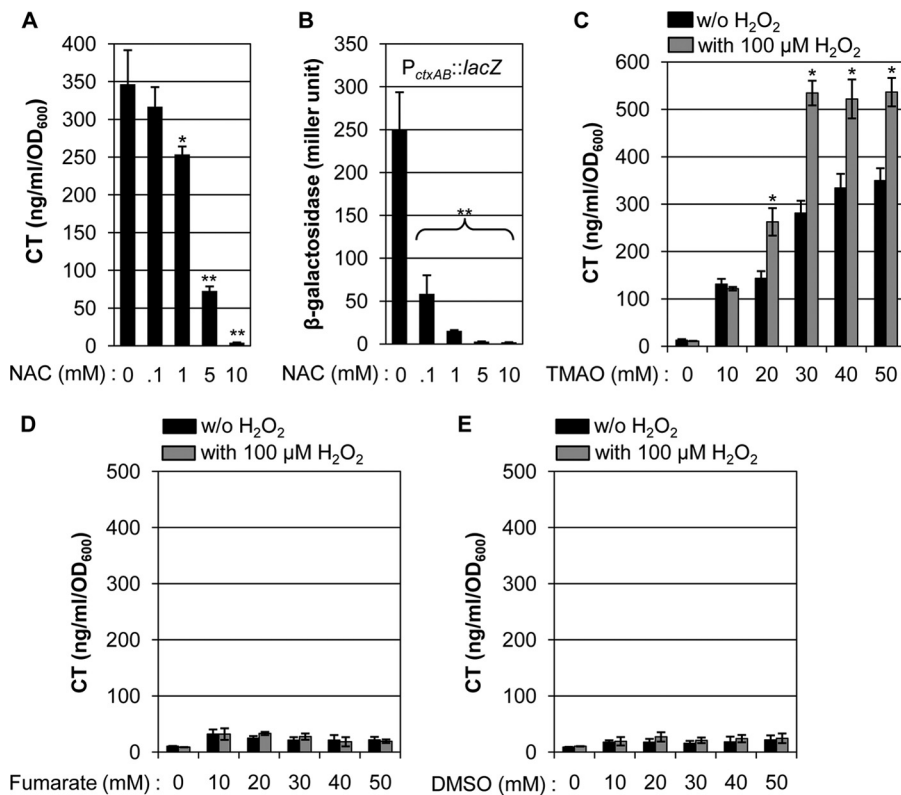

FIGURE 6. **Extraneously added H_2O_2 promotes CT production during anaerobic TMAO respiration.** *A*, effect of the presence of NAC on CT production. N16961 cells were grown anaerobically in LBT for 16 h with the indicated amounts of NAC. Three independent experiments were performed and values of mean $\pm$ S.D. are displayed in each *bar*. *, $p < 0.01$; **, $p < 0.001$ *versus* CT levels detected in cell-free supernatants harvested from cultures with 0 mM NAC. *B*, the effect of the presence of NAC on *ctxAB* promoter activity. An N16961 reporter strain harboring a chromosomal copy of *ctxAB* promoter-*lacZ* fusion was grown anaerobically in LBT in the presence of increasing concentrations of NAC. Bacterial culture conditions were identical to those described in the legend to Fig. 6*A* and β-galactosidase activity was measured as described in the legend to Fig. 1*D*. Three independent experiments were performed and values of mean $\pm$ S.D. are displayed in each *bar*. **, $p < 0.001$ *versus* β-galactosidase activity detected in cells grown with 0 mM NAC. *C–E*, effect of extraneously added H_2O_2 on CT production. LB media with varying concentrations of TMAO (*C*), fumarate (*D*), or DMSO (*E*) were supplemented with no (*black bars*) or 100 μM H_2O_2 (*gray bars*). N16961 was grown anaerobically in each media for 16 h and culture supernatants were collected for CT ELISA. Three independent experiments were performed and values of mean $\pm$ S.D. are displayed in each *bar*. *, $p < 0.01$ *versus* CT levels produced without added H_2O_2.
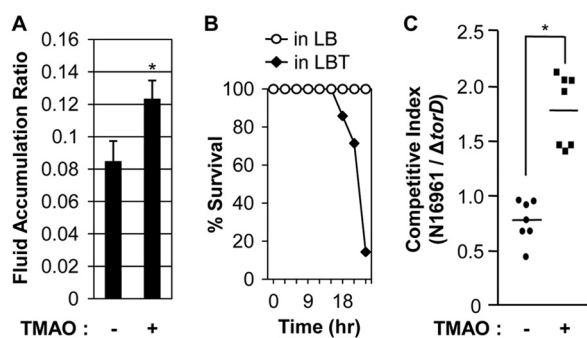
FIGURE 7. **Effects of TMAO on *in vivo* virulence and colonization.** *A*, infant mice (*n* = 7) were infected with N16961 cells (2×10^6 cells) suspended in LB (*left bar*) or LB + 100 mM TMAO (*right bar*). After 24 h, mice were sacrificed and the entire intestines were extracted for weight measurement. Fluid accumulation ratio was calculated as intestine weight divided by (body weight − intestine weight). For infection with TMAO, the increase in FAR was statistically significant (*, $p < 0.005$). *B*, identical set of mice used in experiments described in *panel A* were examined to check their viability every 3 h. Percent survival in each group was plotted with time. *C*, mice were co-infected with an equal number of N16961 and Δ*torD* mutant (1×10^6 cells, each). Again, bacterial cells were resuspended in LB or LB containing 100 mM TMAO. The competitive index represents the ratio of N16961 to Δ*torD* mutant recovered after infection. Seven mice were used for each infection and mean ± S.D. are presented (*, $p < 0.005$ *versus* competitive index obtained from infection with no added TMAO).

mice infected with bacterial suspensions in plain LB survived for 24 h, only one mouse survived at 24 h post-infection when TMAO was added to the inoculum (Fig. 7*B*). These results suggest that *V. cholerae* strains exert more severe virulence to infant mice in the presence of added TMAO.

Our results in Fig. 2*A* demonstrate that wild type N16961, but not the Δ*torD* mutant, exhibited enhanced *in vitro* growth by TMAO respiration. Therefore, we investigated whether *in vivo* colonization of the Δ*torD* mutant is compromised, compared with the wild type strain. To address this issue, we calculated the competitive index between these two strains. Infant mice (*n* = 7) were co-infected with equal numbers of N16961 and Δ*torD* mutant cells re-suspended in LB or LBT (1×10^6 cells each). When TMAO was not added to the inoculum, the level of intestinal colonization by N16961 was slightly less than that of the Δ*torD* mutant, yielding a competitive index of ∼0.77 (Fig. 7*C*, *closed circles*). In contrast, when the mixture of bacterial cells was inoculated with 100 mM TMAO, the number of N16961 cells was higher than that of the mutant cells (Fig. 7*C*, *closed squares*). The competitive index in this set of experiments was ∼1.78 and the difference between the two competitive indexes was statistically significant ($p < 0.005$). Together, these results suggest that the ability to metabolize TMAO may be important not only for *in vivo* virulence but also for intestinal colonization.

DISCUSSION

As a historic enteric pathogen, *V. cholerae* has been extensively investigated for the regulation of virulence factors. For successful colonization and CT production in host intestinal microenvironments, the organism must alter its phenotypic and metabolic properties from those of its natural aquatic habitat. Because the human intestinal environment is largely anaerobic (7, 41), there is a need for the pathogen to utilize chemicals other than oxygen as AEAs for anaerobic growth. *V. cholerae* is

reported to be capable of metabolizing organic amines including TMAO and fumarate under anaerobic growth conditions (15). However, there is a lack of information regarding the effect of anaerobic respiration on bacterial growth or regulated production of virulence factors for an *in vitro* culture system that resembles the human intestinal microenvironment.

CT is the major virulence factor that critically influences *V. cholerae* pathogenesis. Although genetic regulatory systems leading to activation of *ctxAB* gene expression are relatively well established (4, 42, 43), environmental signals that induce CT expression are not clearly defined. The AKI condition, which has been considered as an efficient *in vitro* culture method for CT production, involves a biphasic growth of the 4-h static culture followed by vigorous shaking for 16 h (44, 45). In addition, the volume-to-surface ratio of laboratory flask cultures was reported to play a role in regulating CT production (46). Because these culture methods were all developed by trial and error, why they trigger CT production is still unknown. In this study, we identified a previously undescribed culture condition that induces CT production and investigated the molecular basis of such induction and its relevance for *in vivo* infection.

Our conclusion that CT production was specifically induced when *V. cholerae* grew by anaerobic TMAO respiration stems from the following evidence: (i) CT production was not induced by other AEAs and (ii) Δ*torD* and Δ*tat* mutant strains of N16961 failed to produce CT during TMAO respiration. Because the anaerobic growth of *V. cholerae* was higher with TMAO than with fumarate or DMSO, we postulated that TMAO respiration can provide both a growth advantage to *V. cholerae* under anaerobic conditions and a significantly elevated potential for virulence. Consistent with this notion, the infant mouse infection experiments clearly demonstrated effects of extraneously added TMAO on *in vivo* virulence and competitive intestinal colonization.

In humans, TMAO is produced via an enzyme called flavin-containing monooxygenase, which catalyzes TMA oxidation. TMA is derived from ingested food sources, such as phosphatidylcholine and L-carnitine (47). In a recent study by Wang *et al.*, TMAO was not detected in mice when gut microbiota were suppressed by treatment with antibiotics for 3 weeks (54). The TMAO level was restored after the mouse gut was recolonized by gut microbiota, indicating the key role of gut commensal bacteria for TMAO production (54). As our results showed that CT production could be induced in N16961 with as low as 10 mM TMAO, it seems necessary to determine how much TMAO is present in the human intestine and whether such a level is enough to support both anaerobic growth and CT production of *V. cholerae in vivo*. Furthermore, it would also be of particular interest to examine the correlation between the altered gut microbiota population profiles and differential susceptibility to *V. cholerae* infection. Because TMAO is mainly found in marine environments (48, 49), individuals with a marine diet may have elevated levels of TMAO in their intestine and be at a higher risk for pathogenic *V. cholerae* infection.

Proteins secreted by the Type II secretion system are translocated to the periplasm via the general secretion (SEC) system (50, 51) or TAT system (52). However, our results showed that

CT secretion was not significantly compromised in the Δ*sec* mutant, demonstrating that CT secretion likely occurs independently of the SEC pathway during anaerobic growth by TMAO respiration. This finding was rather unexpected because the SEC pathway was reported to be critical for CT secretion during aerobic growth (35, 36). In a recent study by Zhang and colleagues (22), CT production in a *V. cholerae* mutant deficient in the TAT pathway was only mildly affected during aerobic growth under AKI conditions. This result is also in marked contrast to our finding that CT production was completely abrogated in the Δ*tat* mutant during anaerobic TMAO respiration. Together, these results suggest that CT secretion during anaerobic TMAO respiration may occur following different mechanisms than those operational during aerobic growth.

Our results in Fig. 5 clearly demonstrate that N16961 cells grown anaerobically with TMAO exhibited a strong fluorescent signal when stained with DCF-DA, a ROS detector. Because the fluorescent signal was only detected in cells grown by TMAO respiration, the growth mode that resulted in CT production, we postulated that ROS generated during TMAO respiration would trigger a signal leading to CT production. In support of this hypothesis is the finding that both CT production and *ctxAB* gene transcription decreased in the presence of NAC, a compound that can reduce the availability of cellular ROS. TMAO reductase reduces TMAO to TMA. Because TMA is the only product of TMAO reductase, it was also postulated that TMA might be the signal to induce CT production. However, neither growth enhancement nor CT production was observed when N16961 was grown anaerobically with 50 mM TMA (data not shown). This result further confirms that a signal leading to the CT production (*i.e.* ROS) is generated during TMAO reduction. The level of CT produced during TMAO respiration was substantially elevated when the culture medium was "spiked" with H_2O_2. However, the positive effect of H_2O_2 on CT production was not observed in N16961 grown in plain LB. These results strongly suggest that (i) H_2O_2 alone may not directly induce CT production in *V. cholerae* under anaerobic conditions and (ii) extraneously added H_2O_2 can play a role in expanding the capability of *V. cholerae* to produce CT during TMAO respiration. One possible interpretation would be that anaerobic TMAO respiration contributes to create conditions for CT production and such conditions are further amplified by the addition of extraneous H_2O_2. Interestingly, at up to 0.1% concentration (~28 mM), H_2O_2 was found to increase the TcpA level in another El Tor strain, A1552, during aerobic growth in LB (53). In contrast, our results showed that only 100 μM H_2O_2 was enough to promote maximum CT production. It will be necessary to address (i) how much ROS is generated during TMAO respiration, (ii) how potent is it to transduce virulence inducing signals, and (iii) what is the mode of signal transduction. Because CT subunits A and B do not contain the twin arginine motif, a precise mechanism by which CT secretion occurs in association with the activated TAT pathway also needs to be elucidated.

In conclusion, we explored anaerobiosis-induced changes in growth and virulence properties of *V. cholerae*. Most importantly, we proposed a mechanistic basis for a strict dependence
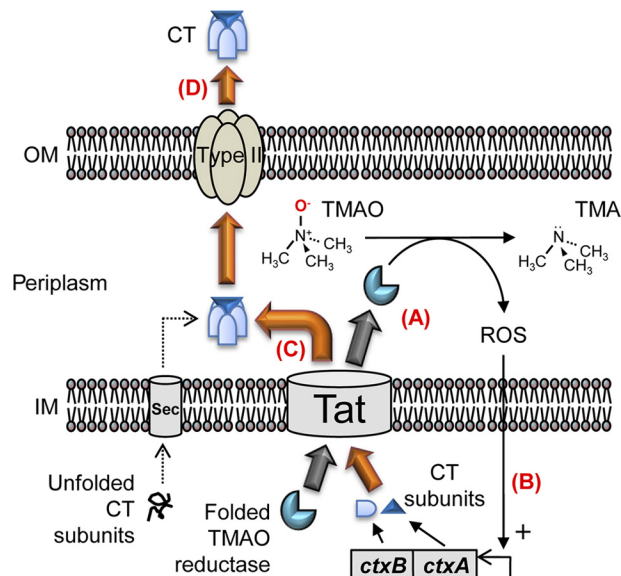

FIGURE 8. **Summary of potential mechanisms by which CT is produced during anaerobic TMAO respiration.** *A,* in the presence of TMAO, the TAT pathway is activated to translocate TMAO reductase to the periplasmic space. *B,* ROS, generated during TMAO reduction to TMA, can stimulate a signal to activate *ctxAB* gene transcription for a mechanism that needs to be further investigated. *C,* presumably, CT subunits take advantage of the activated TAT pathway to be translocated into the periplasm. *D,* CT is excreted into the environmental milieu via the type II secretion pathway. For a simple presentation, the type II secretion apparatus present only in the outer membrane portion is depicted.

of CT production on the anaerobic TMAO respiration (summarized in Fig. 8). To identify effective strategies to cope with *V. cholerae* infection, a molecular level understanding of its virulence modulation is necessary. Our results revealed a previously unidentified mechanism for CT production under conditions that likely mimic the environments of the human intestine and therefore, we anticipate that results provided in this study will stimulate further investigations to reduce the severity of intestinal infections caused by this clinically important human pathogen.

REFERENCES

1. Faruque, S. M., Albert, M. J., and Mekalanos, J. J. (1998) Epidemiology, genetics, and ecology of toxigenic *Vibrio cholerae*. *Microbiol. Mol. Biol. Rev.* **62,** 1301–1314
2. Piarroux, R., Barrais, R., Faucher, B., Haus, R., Piarroux, M., Gaudart, J., Magloire, R., and Raoult, D. (2011) Understanding the cholera epidemic, Haiti. *Emerg. Infect. Dis.* **17,** 1161–1168
3. Yoon, S. S., Coakley, R., Lau, G. W., Lymar, S. V., Gaston, B., Karabulut, A. C., Hennigan, R. F., Hwang, S. H., Buettner, G., Schurr, M. J., Mortensen, J. E., Burns, J. L., Speert, D., Boucher, R. C., and Hassett, D. J. (2006) Anaerobic killing of mucoid *Pseudomonas aeruginosa* by acidified nitrite derivatives under cystic fibrosis airway conditions. *J. Clin. Invest.* **116,** 436–446
4. Matson, J. S., Withey, J. H., and DiRita, V. J. (2007) Regulatory networks controlling *Vibrio cholerae* virulence gene expression. *Infect. Immun.* **75,** 5542–5549
5. Spangler, B. D. (1992) Structure and function of cholera toxin and the related *Escherichia coli* heat-labile enterotoxin. *Microbiol. Rev.* **56,** 622–647
6. Iredell, J. R., and Manning, P. A. (1994) The toxin-co-regulated pilus of *Vibrio cholerae* O1. A model for type 4 pilus biogenesis? *Trends Microbiol.* **2,** 187–192
7. Bäckhed, F., Ley, R. E., Sonnenburg, J. L., Peterson, D. A., and Gordon, J. I.

(2005) Host-bacterial mutualism in the human intestine. *Science* **307,** 1915–1920

8. Marrero, K., Sánchez, A., Rodríguez-Ulloa, A., González, L. J., Castellanos-Serra, L., Paz-Lago, D., Campos, J., Rodríguez, B. L., Suzarte, E., Ledón, T., Padrón, G., and Fando, R. (2009) Anaerobic growth promotes synthesis of colonization factors encoded at the *Vibrio* pathogenicity island in *Vibrio cholerae* El Tor. *Res. Microbiol.* **160,** 48–56

9. Häse, C. C., and Mekalanos, J. J. (1998) TcpP protein is a positive regulator of virulence gene expression in *Vibrio cholerae. Proc. Natl. Acad. Sci. U.S.A.* **95,** 730–734

10. Liu, Z., Yang, M., Peterfreund, G. L., Tsou, A. M., Selamoglu, N., Daldal, F., Zhong, Z., Kan, B., and Zhu, J. (2011) *Vibrio cholerae* anaerobic induction of virulence gene expression is controlled by thiol-based switches of virulence regulator AphB. *Proc. Natl. Acad. Sci. U.S.A.* **108,** 810–815

11. Kovacikova, G., Lin, W., and Skorupski, K. (2010) The LysR-type virulence activator AphB regulates the expression of genes in *Vibrio cholerae* in response to low pH and anaerobiosis. *J. Bacteriol.* **192,** 4181–4191

12. Nobechi, K. (1925) Contributions to the knowledge of *Vibrio cholerae* I. Fermentation of carbohydrates and polyatomic alcohols by *Vibrio cholerae. J. Bacteriol.* **10,** 197–215

13. Konishi, K., Yamagishi, T., and Sakamoto, K. (1981) A *Halophilic vibrio* isolated from a case of chronic cholecystitis. *Microbiol. Immunol.* **25,** 1221–1228

14. Nicholls, K. M., Lee, J. V., and Donovan, T. J. (1976) An evaluation of commercial thiosulfate citrate bile salt sucrose agar (TCBS). *J. Appl. Bacteriol.* **41,** 265–269

15. Braun, M., and Thöny-Meyer, L. (2005) Cytochrome c maturation and the physiological role of c-type cytochromes in *Vibrio cholerae. J. Bacteriol.* **187,** 5996–6004

16. Lee, K. M., Go, J., Yoon, M. Y., Park, Y., Kim, S. C., Yong, D. E., and Yoon, S. S. (2012) Vitamin B12-mediated restoration of defective anaerobic growth leads to reduced biofilm formation in *Pseudomonas aeruginosa. Infect. Immun.* **80,** 1639–1649

17. Gardel, C. L., and Mekalanos, J. J. (1994) Regulation of cholera toxin by temperature, pH, and osmolarity. *Methods Enzymol.* **235,** 517–526

18. Miyata, S. T., Kitaoka, M., Brooks, T. M., McAuley, S. B., and Pukatzki, S. (2011) *Vibrio cholerae* requires the type VI secretion system virulence factor VasX to kill *Dictyostelium discoideum. Infect. Immun.* **79,** 2941–2949

19. Lee, K. M., Yoon, M. Y., Park, Y., Lee, J. H., and Yoon, S. S. (2011) Anaerobiosis-induced loss of cytotoxicity is due to inactivation of quorum sensing in *Pseudomonas aeruginosa. Infect. Immun.* **79,** 2792–2800

20. Philippe, N., Alcaraz, J. P., Coursange, E., Geiselmann, J., and Schneider, D. (2004) Improvement of pCVD442, a suicide plasmid for gene allele exchange in bacteria. *Plasmid* **51,** 246–255

21. Yoon, M. Y., Lee, K. M., Park, Y., and Yoon, S. S. (2011) Contribution of cell elongation to the biofilm formation of *Pseudomonas aeruginosa* during anaerobic respiration. *PLoS ONE* **6,** e16105

22. Zhang, L., Zhu, Z., Jing, H., Zhang, J., Xiong, Y., Yan, M., Gao, S., Wu, L. F., Xu, J., and Kan, B. (2009) Pleiotropic effects of the twin arginine translocation system on biofilm formation, colonization, and virulence in *Vibrio cholerae. BMC Microbiol.* **9,** 114

23. Heidelberg, J. F., Eisen, J. A., Nelson, W. C., Clayton, R. A., Gwinn, M. L., Dodson, R. J., Haft, D. H., Hickey, E. K., Peterson, J. D., Umayam, L., Gill, S. R., Nelson, K. E., Read, T. D., Tettelin, H., Richardson, D., Ermolaeva, M. D., Vamathevan, J., Bass, S., Qin, H., Dragoi, I., Sellers, P., McDonald, L., Utterback, T., Fleishmann, R. D., Nierman, W. C., White, O., Salzberg, S. L., Smith, H. O., Colwell, R. R., Mekalanos, J. J., Venter, J. C., and Fraser, C. M. (2000) DNA sequence of both chromosomes of the cholera pathogen *Vibrio cholerae. Nature* **406,** 477–483

24. Michalski, J., Galen, J. E., Fasano, A., and Kaper, J. B. (1993) CVD110, an attenuated *Vibrio cholerae* O1 El Tor live oral vaccine strain. *Infect. Immun.* **61,** 4462–4468

25. Pommier, J., Méjean, V., Giordano, G., and Iobbi-Nivol, C. (1998) TorD, a cytoplasmic chaperone that interacts with the unfolded trimethylamine N-oxide reductase enzyme (TorA) in *Escherichia coli. J. Biol. Chem.* **273,** 16615–16620

26. Layer, G., Verfürth, K., Mahlitz, E., and Jahn, D. (2002) Oxygen-indepen-

dent coproporphyrinogen-III oxidase HemN from *Escherichia coli. J. Biol. Chem.* **277,** 34136–34142

27. Al-Sheboul, S., and Saffarini, D. (2011) Identification and analysis of the *Shewanella oneidensis* major oxygen-independent coproporphyrinogen III oxidase gene. *Anaerobe* **17,** 501–505

28. Dos Santos, J. P., Iobbi-Nivol, C., Couillault, C., Giordano, G., and Méjean, V. (1998) Molecular analysis of the trimethylamine N-oxide (TMAO) reductase respiratory system from a *Shewanella* species. *J. Mol. Biol.* **284,** 421–433

29. Santini, C. L., Ize, B., Chanal, A., Müller, M., Giordano, G., and Wu, L. F. (1998) A novel sec-independent periplasmic protein translocation pathway in *Escherichia coli. EMBO J.* **17,** 101–112

30. Lee, P. A., Tullman-Ercek, D., and Georgiou, G. (2006) The bacterial twin arginine translocation pathway. *Annu. Rev. Microbiol.* **60,** 373–395

31. Méjean, V., Iobbi-Nivol, C., Lepelletier, M., Giordano, G., Chippaux, M., and Pascal, M. C. (1994) TMAO anaerobic respiration in *Escherichia coli.* Involvement of the tor operon. *Mol. Microbiol.* **11,** 1169–1179

32. Gon, S., Giudici-Orticoni, M. T., Méjean, V., and Iobbi-Nivol, C. (2001) Electron transfer and binding of the c-type cytochrome TorC to the trimethylamine N-oxide reductase in *Escherichia coli. J. Biol. Chem.* **276,** 11545–11551

33. Johnson, T. L., Abendroth, J., Hol, W. G., and Sandkvist, M. (2006) Type II secretion. From structure to function. *FEMS Microbiol. Lett.* **255,** 175–186

34. Cianciotto, N. P. (2005) Type II secretion. A protein secretion system for all seasons. *Trends Microbiol.* **13,** 581–588

35. Sandkvist, M., Bagdasarian, M., and Howard, S. P. (2000) Characterization of the multimeric Eps complex required for cholera toxin secretion. *Int. J. Med. Microbiol.* **290,** 345–350

36. Sandkvist, M., Michel, L. O., Hough, L. P., Morales, V. M., Bagdasarian, M., Koomey, M., and DiRita, V. J. (1997) General secretion pathway (eps) genes required for toxin secretion and outer membrane biogenesis in *Vibrio cholerae. J. Bacteriol.* **179,** 6994–7003

37. Barrett, E. L., and Kwan, H. S. (1985) Bacterial reduction of trimethylamine oxide. *Annu. Rev. Microbiol.* **39,** 131–149

38. McCrindle, S. L., Kappler, U., and McEwan, A. G. (2005) Microbial dimethylsulfoxide and trimethylamine N-oxide respiration. *Adv. Microb. Physiol.* **50,** 147–198

39. Ilbert, M., Méjean, V., Giudici-Orticoni, M. T., Samama, J. P., and Iobbi-Nivol, C. (2003) Involvement of a mate chaperone (TorD) in the maturation pathway of molybdoenzyme TorA. *J. Biol. Chem.* **278,** 28787–28792

40. Chandel, N. S., Trzyna, W. C., McClintock, D. S., and Schumacker, P. T. (2000) Role of oxidants in NF-κB activation and TNF-α gene transcription induced by hypoxia and endotoxin. *J. Immunol.* **165,** 1013–1021

41. Taylor, C. T., and Colgan, S. P. (2007) Hypoxia and gastrointestinal disease. *J. Mol. Med.* **85,** 1295–1300

42. DiRita, V. J. (1992) Coordinate expression of virulence genes by ToxR in *Vibrio cholerae. Mol. Microbiol.* **6,** 451–458

43. Klose, K. E. (2001) Regulation of virulence in *Vibrio cholerae. Int. J. Med. Microbiol.* **291,** 81–88

44. Iwanaga, M., Yamamoto, K., Higa, N., Ichinose, Y., Nakasone, N., and Tanabe, M. (1986) Culture conditions for stimulating cholera toxin production by *Vibrio cholerae* O1 El Tor. *Microbiol. Immunol.* **30,** 1075–1083

45. Iwanaga, M., and Yamamoto, K. (1985) New medium for the production of cholera toxin by *Vibrio cholerae* O1 biotype El Tor. *J. Clin. Microbiol.* **22,** 405–408

46. Sánchez, J., Medina, G., Buhse, T., Holmgren, J., and Soberón-Chavez, G. (2004) Expression of cholera toxin under non-AKI conditions in *Vibrio cholerae* El Tor induced by increasing the exposed surface of cultures. *J. Bacteriol.* **186,** 1355–1361

47. Lang, D. H., Yeung, C. K., Peter, R. M., Ibarra, C., Gasser, R., Itagaki, K., Philpot, R. M., and Rettie, A. E. (1998) Isoform specificity of trimethylamine N-oxygenation by human flavin-containing monooxygenase (FMO) and P450 enzymes. Selective catalysis by FMO3. *Biochem. Pharmacol.* **56,** 1005–1012

48. Martinez, I., Bathen, T., Standal, I. B., Halvorsen, J., Aursand, M., Gribbestad, I. S., and Axelson, D. E. (2005) Bioactive compounds in cod (*Gadus morhua*) products and suitability of ^{1}H NMR metabolite profiling for clas-

sification of the products using multivariate data analyses. *J. Agric. Food Chem.* **53,** 6889–6895

49. Bordi, C., Ansaldi, M., Gon, S., Jourlin-Castelli, C., Iobbi-Nivol, C., and Méjean, V. (2004) Genes regulated by TorR, the trimethylamine oxide response regulator of *Shewanella oneidensis. J. Bacteriol.* **186,** 4502–4509

50. Pugsley, A. P. (1993) The complete general secretory pathway in Gram-negative bacteria. *Microbiol. Rev.* **57,** 50–108

51. Desvaux, M., Parham, N. J., Scott-Tucker, A., and Henderson, I. R. (2004) The general secretory pathway. A general misnomer? *Trends Microbiol.* **12,** 306–309

52. Voulhoux, R., Ball, G., Ize, B., Vasil, M. L., Lazdunski, A., Wu, L. F., and Filloux, A. (2001) Involvement of the twin arginine translocation system in protein secretion via the type II pathway. *EMBO J.* **20,** 6735–6741

53. Valeru, S. P., Rompikuntal, P. K., Ishikawa, T., Vaitkevicius, K., Sjöling, A., Dolganov, N., Zhu, J., Schoolnik, G., and Wai, S. N. (2009) Role of melanin pigment in expression of *Vibrio cholerae* virulence factors. *Infect. Immun.* **77,** 935–942

54. Wang, Z., Klipfell, E., Bennett, B. J., Koeth, R., Levison, B. S., Dugar, B., Feldstein, A. E., Britt, E. B., Fu, X., Chung, Y. M., Wu, Y., Schauer, P., Smith, J. D., Allayee, H., Tang, W. H., DiDonato, J. A., Lusis, A. J., and Hazen, S. L. (2011) Gut flora metabolism of phosphatidylcholine promotes cardiovascular disease. *Nature* **472,** 57–63